Medical Engineering & Physics 34 (2012) 906–913

Contents lists available at SciVerse ScienceDirect

Medical Engineering & Physics

journal homepage: www.elsevier.com/locate/medengphy

Prediction of visceral response to multi-directional loading as measured by the chestband

Jason J. Hallman[a,b,*], Narayan Yoganandan[a,b], Frank A. Pintar[a,b]

[a] Department of Neurosurgery, Medical College of Wisconsin, Milwaukee, WI, USA
[b] Zablocki VA Medical Center, Milwaukee, WI, USA

ARTICLE INFO

Article history:
Received 8 June 2011
Received in revised form 6 October 2011
Accepted 11 October 2011

Keywords:
Finite element
Injury biomechanics
Trauma
Thorax
Abdomen
Chestband

ABSTRACT

Thoracic and abdominal injury outcomes are correlated to chestband-derived uniaxial metrics in post-mortem human specimen (PMHS) experiments. Yet, uniaxial metrics may neglect deformations remote from the measurement site which still may be relevant to injury risk in motor vehicle crashes. Using 2D chestband contours from PMHS experiments, visceral strain and strain energy density responses were examined using a planar viscoelastic finite element model. The model was exercised by applying to the periphery 21 subject-specific PMHS chestband deformation patterns representing four boundary conditions: (a) lateral impact with close-proximity torso airbag, (b) stationary close-proximity torso airbag loading, (c) flat rigid lateral impact, and (d) antero-lateral oblique rigid impact. ANOVA determined that mean peak responses were dependent on boundary condition ($p < 0.002$). Using matched-pair experiment injury outcomes, 50% risk of visceral trauma corresponded to localized strain and strain energy density of 1.55 and 33.0 kJ/m^3 ($p < 0.1$). Although strains were large, model response demonstrated sensitivity to impact boundary conditions and observed PMHS trauma. This model formulation is useful for comparative examination of injury risk from torso deformations measured experimentally using the chestband device.

1. Introduction

During blunt lateral impact to the thorax and abdomen, external deflection has been identified as a correlate to resulting injury. With tests utilizing post-mortem human specimens (PMHS) and animal models, deflections have been measured using depth-limited impactors [1], post-experiment digitization of videography [2], invasive linear displacement transducers [3], and "chestband" transducers [4]. The chestband device consists of a flexible steel belt instrumented with resistive strain gages in an axially compensated Wheatstone bridge configuration [5]. Bridge outputs, representing band curvature at underlying points, are post-processed with cubic spline interpolation into two-dimensional (2D) closed contours for each sample time. The post-processing software RBandPC (ver. 3.0, Conrad Technologies, Inc., Washington, DC, available from the US Department of Transportation) was validated using an anthropomorphic test device in sled impacts [6].

Recent lateral impact studies with the chestband have identified complex multidirectional deformation patterns induced by narrow object intrusion [7] or torso side airbag interaction [8]. With these complex deformations, the relationship between transient localized deflections and injury risk to underlying anatomic structures may not be apparent. For example, a study employing PMHS experiments with close-proximity side airbags identified postero-lateral and lateral deflections during impact [8]. While select test specimens also sustained visceral trauma, the causal deformation could not be identified. Therefore, the optimal transducer location for predicting these injuries from external measurements in an anthropomorphic test dummy (ATD) could not be determined. To address this question, the present study details the development of a novel viscoelastic finite element (FE) model to relate internal visceral response and external biomechanics. This planar model, coupled with experimentally derived planar chestband contour results, may quantify the relationship between external deformation characteristics and visceral injury risk in order to develop thoracic injury metrics and direct transducer placement within an ATD chest cross-section.

2. Methods

The FE model was developed from imaging data produced by the Visible Human Project (National Library of Medicine, National Institutes of Health, Bethesda, MD). High resolution axial

* Corresponding author at: Department of Neurosurgery, Medical College of Wisconsin, VA Medical Center – Research 151, 5000, W National Avenue, Milwaukee, WI 53295, USA. Tel.: +1 414 384 2000x41534; fax: +1 414 384 3493.
E-mail address: jhallman@mcw.edu (J.J. Hallman).

1350-4533/$ – see front matter. Published by Elsevier Ltd on behalf of IPEM.
doi:10.1016/j.medengphy.2011.10.006

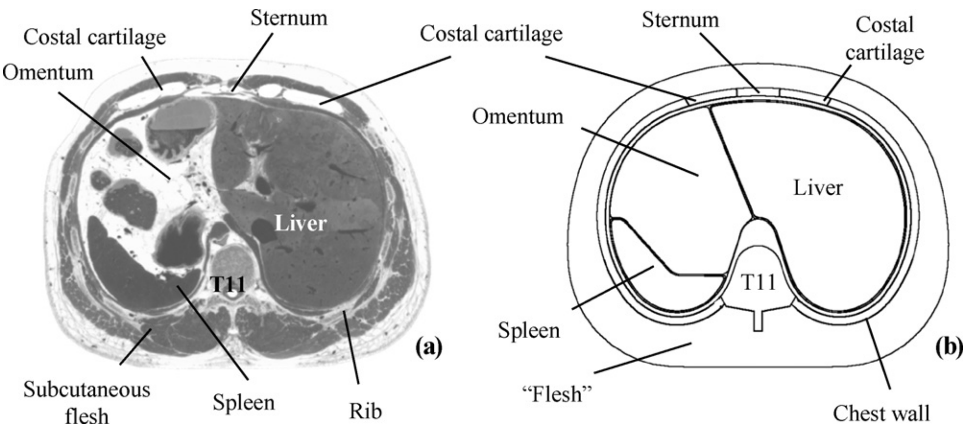

Fig. 1. Geometry of (a) model source image and (b) resulting feature boundaries.

cryomicrotome images were acquired from an adult male donor through a process previously described [9]. Uncompressed images corresponding to the thorax and abdomen were imported into imaging threshold software (Mimics, Materialise, Leuven, Belgium). After the image corresponding to the T11 vertebral body was identified (Fig. 1a), key anatomic structures were segmented to create boundary curves for the following features: vertebral body, chest wall, sternum, liver, spleen, diaphragm, omentum and hollow intra-abdominal structures, and external "flesh" tissue (Fig. 1b).

2.1. Mesh density

The geometry was discretized into four-node shell elements using the LS-DYNA preprocessor LS-PrePost (Livermore Software Technology Corporation, Livermore, CA) for computations employing plane strain formulation. An initial mesh density study determined element size for this analysis [10]. External flesh elements averaged 5 mm side length, while elements composing the chest wall and visceral contents, i.e., liver, spleen, and omentum, averaged 2.5 mm side length. The final mesh (Fig. 2) was composed of 11,438 elements, 91.1% of which were characterized by aspect ratios <2; 99.3% of element quadratic angles were between 45° and 135°. Self-contacts were defined between all nodes to prevent self-penetration. Frictionless surface-to-surface contacts were defined between all intra-abdominal contents and the chest wall. To account for relative motion between layers of subcutaneous tissues [11], a single sliding-only contact was defined between the subcutaneous flesh and the chest wall.

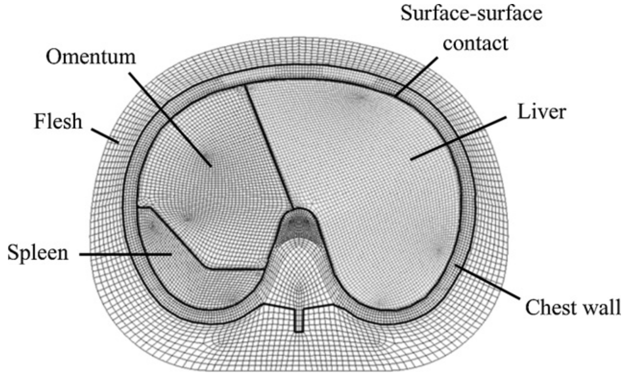

Fig. 2. Mesh density for the planar model.

2.2. Material properties

Material properties were selected according to the literature and from iterative tuning to published biomechanical experiments [12–17]. Material models were assumed as follows: The vertebral body and sternum, rigid; the chest wall, costal cartilage, and costovertebral tissues, linear elastic; flesh, liver, spleen, diaphragm, and omentum, linear viscoelastic. Final properties are given in Table 1.

Because ribs were oblique with respect to the model section plane, a generalized chest wall of 8 mm thickness represented ribs as well as overlying and intercostal tissues (Figs. 1 and 2). The material properties for this generalized chest wall were determined by scaling rib material properties from the literature according to two parameters: (i) fractional representation of bone in the total chest wall cross-section and (ii) bending thickness variation between the total chest wall and ribs. From elementary beam theory, the relationship between these parameters was determined according to Eq. (1):

$$E_{\text{wall}} = \frac{A_{\text{ribs}}}{A_{\text{wall}}}\left(\frac{h_{\text{rib}}}{h_{\text{wall}}}\right)^3 E_{\text{rib}} \tag{1}$$

where h_{rib} and h_{wall} represent the rib and chest wall bending thicknesses, E_{rib} represents the experimentally measured rib bending modulus [18], and A_{ribs} and A_{wall} represent the total cross-sectional areas of the ribs and chest wall in the human [19,20].

2.3. Validation

Model response was validated to individual organ/tissue experiments and to lateral and oblique PMHS pendulum impacts (Fig. 3). Liver response was validated to dynamic compression tests in

Table 1
Material properties chosen for the planar model.

Material	ρ (kg/m^3)	K/E[a] (MPa)	G_0 (MPa)	G_∞ (MPa)	Poisson ratio
Flesh	1100	0.5	0.350	0.170	
Chest wall	1310	350	–	–	0.3
Costal cartilage	1200	25	–	–	0.4
Costovertebral junction	1200	50	–	–	0.4
Omentum	1100	0.5	0.054	0.040	–
Diaphragm	1100	0.5	0.400	0.100	–
Liver: parenchyma	1100	0.5	0.230	0.044	–
Liver: capsule	1100	–	0.300	0.065	–
Spleen: parenchyma	1100	0.5	0.069	0.013	–
Spleen: capsule	1100	–‘	0.345	0.065	–

[a] Tabulated value indicates K and E for viscoelastic and elastic materials, respectively.